Particle Radiation Therapy for Liver Tumors: Simulation and Treatment Planning

10

Matthew Knecht, MD, Andrew Wroe, PhD
and Gary Y. Yang, MD

10.1 Introduction

After discovery of X-rays in 1895 and their subsequent therapeutic use in skin lesions shortly thereafter in 1896, research has been undertaken to understand and minimize the risks of radiation therapy to normal tissues, while still maintaining tumoricidal doses. As a part of the progression toward improving the therapeutic window, Dr. Ernest Lawrence developed the ability to accelerate ions, and one of his students, Dr. Robert Wilson, wrote the seminal paper hypothesizing the medical use of ion beam therapy in 1946 [1]. In that paper, he showed the graph indicating the Bragg Peak, and discussed the improved penumbra offered by protons over electrons.

Heavy charged particles (i.e., protons and heavier ions) deposit energy primarily through coulombic interactions with orbital electrons and to a small degree through nuclear collisions. As described by Wilson, heavy charged particles deposit significantly more energy in the final portion of their path length in a region called the Bragg peak, which for protons is of the order of a few millimeters at the 90% dose level. This leads to lower entrance doses than photon-based techniques, which allows for fewer beams to be used than with photon techniques, and no primary proton dose beyond the Bragg peak. Other advantageous physical properties of charged particle beams include tighter penumbra at depths less than 15 cm [2, 3] and uniform dose delivery across the target volume with the use of a spread out Bragg peak (SOBP) (Fig. 10.1).

The first clinical use of an ion beam was undertaken by investigators at Berkeley in 1954. Further research included pituitary adenoma treatments at Harvard in 1963, and the first hospital-based proton facility opened at Loma Linda in 1990. These proton centers were developed utilizing passively scattered proton beams that treat the entire tumor volume with a uniform dose at a given time. Subsequent advances in beam delivery techniques have led to the development of proton pencil beam scanning systems that utilize a narrow proton beam and scanning magnets to paint a dose over the desired target. Beyond protons, other particles, such as carbon, are in medical use and showing encouraging initial clinical outcomes.

External beam radiation therapy for liver tumors was initially limited by the high risk of radiation-induced liver disease (RILD) especially since many primary liver tumors occur in the setting of an already cirrhotic liver. As technologic improvements allowed for increasingly

M. Knecht · A. Wroe
Department of Radiation Medicine, Loma Linda University Health, 11234 Anderson St, Suite A-875, Loma Linda, CA 92354, USA
e-mail: mknecht@llu.edu

A. Wroe
e-mail: awroe@llu.edu

G.Y. Yang (✉)
Department of Radiation Medicine, Loma Linda University Health, 11234 Anderson St, Suite B-121, Loma Linda, CA 92354, USA
e-mail: gyang@llu.edu

J. Meyer and T.E. Schefter (eds.), *Radiation Therapy for Liver Tumors*,
DOI 10.1007/978-3-319-54531-8_10

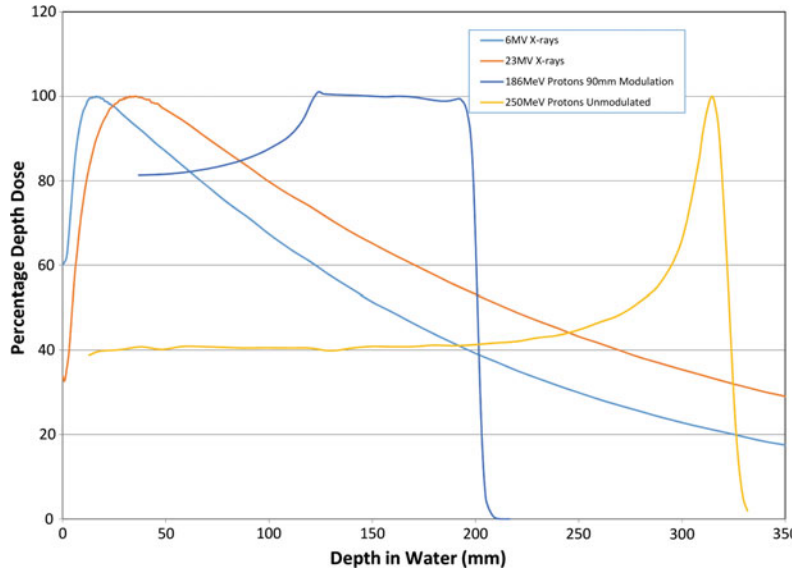

Fig. 10.1 Depth dose profiles for 6 and 23 MV X-rays for comparison with a 90-mm modulated 186 MeV proton beam and an unmodulated 250 MeV proton beam

conformal radiation delivery, photon-based techniques became a viable treatment modality for liver tumors. Particle therapy allows for sparing of low and intermediate radiation dose relative to photon therapy with lower integral dose, an ability to avoid critical structures altogether through the use of fewer beams, no exit dose, and potentially tighter penumbra, thus providing an even wider therapeutic window when treating liver tumors.

The goal of this chapter will be to familiarize the reader with the pertinent practical aspects of ion beam therapy in the treatment of liver patients. The primary particle discussed will be protons, with mention of carbon ions, and the issues surrounding clinical deployment of these ions.

10.2 Patient Selection

When considering particle therapy for liver tumors, many of the selection criteria are disease- and liver function-specific and are thus similar to photon techniques; however, the lower integral dose provided by particle therapy is theorized to expand the therapeutic window, and thus expand patient selection. Basic eligibility for local treatment and thus criteria for the reported phase II trials evaluating particle therapy for hepatocellular carcinoma (HCC) include histologic or imaging diagnosis of HCC limited to the liver (including patients with vessel thrombus), adequate hepatic function, Child-Turcotte-Pugh (CTP) class A or B cirrhosis, Eastern Cooperative Oncology Group (ECOG) performance status 0–2, with three or fewer lesions, who were not eligible at that time for resection or transplant [4–8].

Further considerations which favor selecting radiation therapy over other treatment modalities include the tumor size, tumor thrombus, and central location within the liver. Other modalities used to ablate liver neoplasms, discussed elsewhere in this text, have difficulty treating tumors for a number of different technical factors (thermoablation due to heat sink effect of large vessels and larger tumor size, transarterial chemoembolization [TACE] due to tumor thrombus and blood flow). However, ablative radiation can deliver tumorcidal treatment in these areas and need only meet the dose constraints of the normal organs, thus making it a good treatment option in such cases.

The utility of selecting particle therapy over photon-based techniques comes as particle therapy can allow for further sparing of liver tissue due to reduced low- and intermediate -dose regions (see Fig. 10.2). Thus far, these issues have been explored by retrospective reviews and mathematical modeling showing that for larger tumors

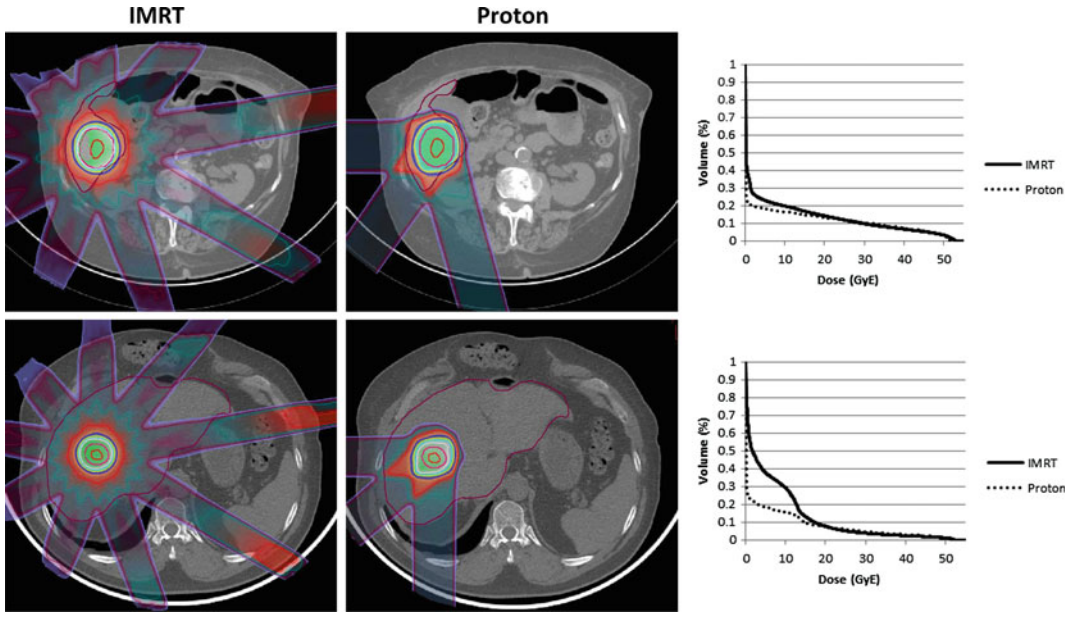

Fig. 10.2 This figure shows nine beam IMRT plans and three beam, passively scattered proton plans for an inferior liver lesion, *upper row*, and a dome lesion, *lower row*. Low and intermediate dose sparing is shown in the liver dose volume histograms, corresponding to the treatment plans in each row

(>5 cm) and for tumors in the central locations larger than 3 cm there is significant sparing of liver tissue with proton therapy [9]. Furthermore, retrospective reviews treating patients with tumors larger than 10 cm [10], CTP class C [11], and portal vein thrombosis [12] provide initial evidence for proton therapy as a treatment modality for these challenging scenarios.

There are several conditions which led to patients being excluded from the reported phase II studies. These included unstable ascites and proximity to gastrointestinal (GI) structures. As ascitic fluid volume changes, the proton path length to the target changes as well which, if unaccounted for, can lead to proton range errors and unacceptable dose coverage of the target.

10.3 Immobilization and Simulation

The goal of immobilization is to provide a stable system by which the patient can be reproducibly set up for treatment on a daily basis. For liver tumors the reproducibility of setup is reflected in the magnitude of the combination an internal target volume (ITV) and planning target volume (PTV) expansions. The ITV expansion reflects the estimated intrafractional motion and the PTV accounts for daily patient setup variability [13] and in the case of protons, beam-specific uncertainties, including range uncertainty.

At Loma Linda University James M. Slater, MD Proton Treatment and Research Center (JMSPTRC), a cylindrical whole body immobilizer or pod system was adapted from 1980s Switzerland's Paul Scherrer Institute (**PSI**) immobilization for pion beam treatments [14] (see Fig. 10.3). Initially developed as a patient-specific polyvinyl chloride pod, it has been upgraded to utilize a generic carbon fiber pod with a patient-specific insert [14, 15]. During simulation the patient lies in the patient-specific insert (which is indexed to the carbon fiber pod) while self-expanding foam is poured around the patient to create the external portion of patient immobilization. This methodology provides a customized whole body immobilization of the

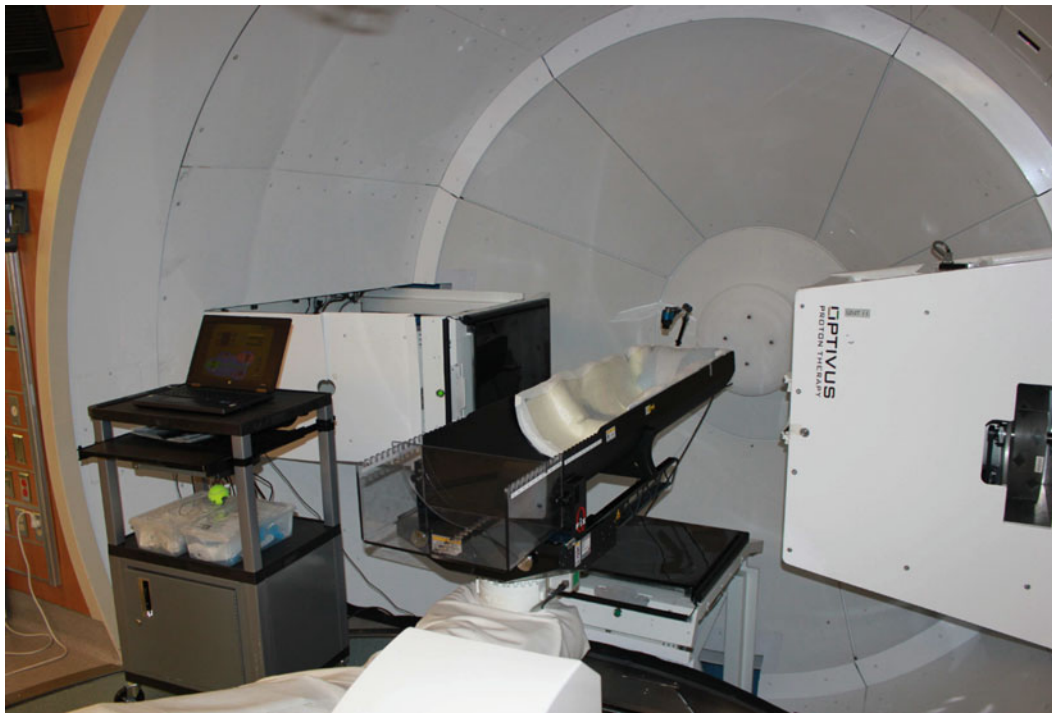

Fig. 10.3 Patient setup at Loma Linda utilizing pod immobilization and SDX for active breath management for treatment of liver tumors

patient allowing for improved stability and reproducibility of setup. Additionally for proton and ion therapy, this system also produces a reproducible external contour of the patient ensuring a reproducible water equivalent path length (WPL) for beams that traverse the immobilization system. Other immobilization options include alpha cradles, vac-lock bags and stereotactic vac-lock bags, however, such systems generally do not ensure a reproducible patient external contour and WPL.

For targets in the abdomen, it is also important to consider respiratory motion in treatment planning and delivery, and thus address this matter during the simulation process. While motion can be tracked and gated with the use of implanted fiducials and external camera systems, the implementation of this can be difficult in proton and ion therapy. This is because while tracking can ensure accurate placement of the target relative to the beam central axis, respiratory motion can result in changes to the water equivalent depth of the target, leading to errors in Bragg peak positioning and underdosing of the target and/or overdosing of surrounding structures. Another option is to reduce target motion using active breathing control, voluntary breath hold, belt systems and spirometric devices. At the JMSPTRC target motion is reduced with a spirometry device (SDX^{TM} available from Qfix) which ensures a reproducible breath hold. The SDX unit differs from active breathing control systems in that while it monitors the patient's inspiration volume, it does not control it. Rather the patient participates in their treatment via feedback from a video screen representation of their level of inspiration. The patient breathes into a predetermined level of inspiration and then a countdown timer displayed to the patient instructs them on the duration of the breath hold for the given treatment or imaging cycle.

Following immobilization simulation proceeds with a non-contrast CT for treatment planning and a contrast CT for tumor localization, both of which

are taken under deep inspiration breath hold. Fiducials are not employed due to the requirement for an invasive procedure and the dose shadow which results from the use of metallic fiducials [16]. Carbon-coated ceramic and stainless steel fiducials are under investigation as an option to address the dose shadow [17], and currently liquid fiducials are becoming clinically available which can be placed with minimally invasive techniques [18]. If a patient cannot tolerate the use of spirometry device the patient is imaged and treated under free breathing conditions and a 4DCT is utilized to define the extent of tumor motion. This approach is possible for passive scattering proton/ion beam delivery as the beam dimensions are static and can be constructed to encompass the target during all phases of the respiration cycle.

10.4 Treatment Planning and Dosimetry

After patient immobilization and imaging, the goal of treatment planning and dosimetry is to define a target and develop a robust plan to deliver a tumoricidal dose to that volume. The target is defined by the gross tumor volume (GTV), with expansions for the clinical tumor volume (CTV), ITV (for mobile tumors), and PTV. A tumoricidal dose then can be planned with beam number and angle selection, addressing proton-specific treatment planning characteristics and patient setup uncertainty.

As mentioned above, target delineation for proton therapy at JMSPTRC utilizes a planning CT scan under breath hold if tolerated by the patient or free breathing conditions if not, without intravenous contrast. A second CT scan under the same conditions with intravenous contrast is performed to guide target delineation, but is not used for dose calculation. The GTV is then defined as the tumor volume seen on the contrast study with reference to prior diagnostic four-phase CT scans or MRIs.

Beyond the GTV, the CTV is added to encompass subclinical disease. The expansion to create the CTV varies between 0 and 1 cm in the reported phase II trials [4–8], and is added at the discretion of the treating physician. In Radiation Therapy Oncology Group (RTOG) 1112, the CTV is defined as being equal to the GTV except in the following situations where an appropriate expansion is added: non-tumor thrombi, prior TACE cavity, or other prior ablation site. Currently at Loma Linda, trials addressing hepatocellular carcinoma include a 1-cm CTV expansion limited to the liver parenchyma, while there is no GTV-to-CTV expansion on the liver metastasis protocol.

The GTV and CTV are assigned based upon tumor characteristics, while the ITV and PTV are added to account for physical uncertainties during treatment. The concept of an ITV, an additional margin to account for intrafractional, physiologic variation (usually relating to respiration-induced motion), was not widely implemented in the current protocols [4–8] and was often included in the overall PTV expansion. Methods described above are used to quantify or limit the amount of physiologic variation, and as recommended by RTOG 1112, breathing motion management is used if the motion is greater than 5 mm on 4DCT. At Loma Linda, when the SDX spirometry device is used for immobilization, no additional margin is added for ITV.

The concept of a PTV in proton therapy is a combination of the familiar physical setup uncertainty as well as beam-specific considerations. Physical setup uncertainty includes the known daily variation of the setup, immobilization, and daily imaging. At JMSPTRC the combination of full body pod and daily orthogonal kV imaging results in a 5 mm daily setup uncertainty. The second component of the PTV in proton planning is a beam-specific range uncertainty (Fig. 10.4). The PTV is related to the stopping power ratio along the beam path during dose calculation including uncertainties in the patient CT image, uncertainty in the parameterized stoichiometric formula to calculate theoretical CT numbers, deviation in human tissue from ICRU standard tissue, uncertainty in mean excitation energy, and uncertainty due to energy dependence of the stopping power ratio not accounted for by the dose calculation algorithm [19]. Additionally, beam-specific uncertainties

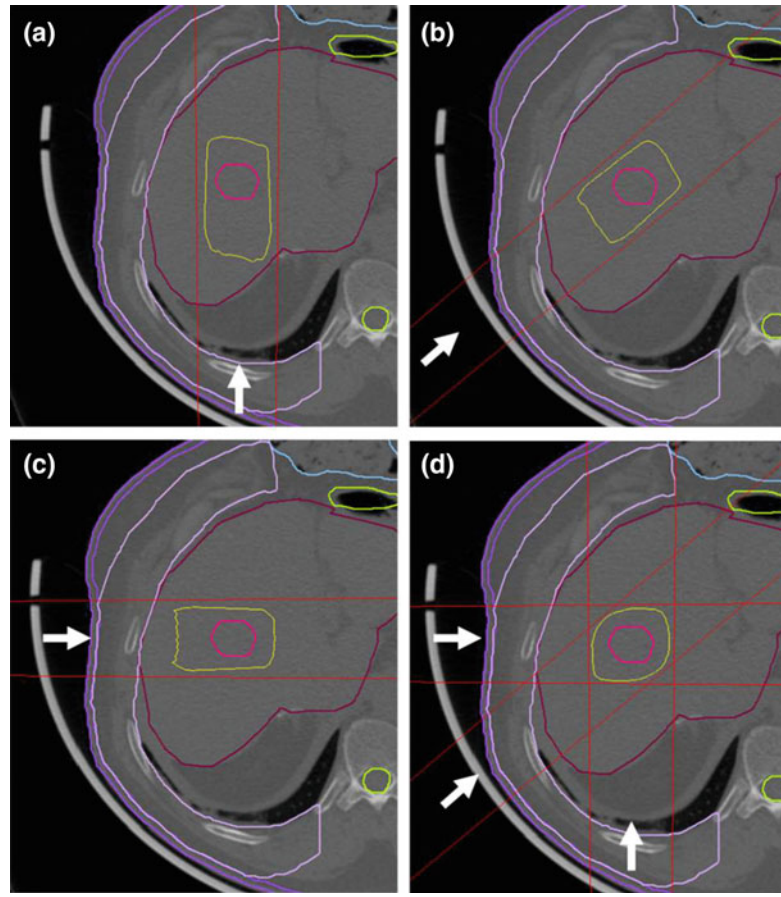

Fig. 10.4 *Panels* **a**, **b,** and **c** show the proton beam-specific PTV as represented by the 90% isodose line, and *panel* **d** shows the combined PTV, *arrows* indicate beam direction

not related to the dose calculation include: commissioning measurement uncertainty, error in compensator design, beam reproducibility, and patient setup [20] also need to be considered. An excellent overview table for range uncertainties and their sources can be found in the Paganetti article [20]. Beam-specific range uncertainty is specified as 3.0–3.5% of the proton range applied to the distal and proximal margins of the target volume to generate a beam-specific PTV. The beam-specific PTV governs the planning for that specific beam with parameters such as beam energy, modulation, compensator design, spot pattern, etc., optimized to ensure coverage of the beam-specific PTV with the prescribed isodose contour.

With regards to proton specific dose constraints there is a significant amount of heterogeneity seen on the current phase II trials though the following constraints can act as a guide: mean liver dose of 13 GyE with a dose of 50 GyE, in 10 fractions per RTOG 1112, V25 < 33% for a prescription of 70.2 GyE in 15 fractions [4], and a mean liver dose of less than or equal to 24 GyE with a prescription of 67.5 GyE in 15 fractions [6]. Currently at Loma Linda, the following constraints are used: for HCC treatment with 70.2 GyE in 15 fractions, liver V25 < 33%; for HCC treatment with GyE in 5 fractions, mean liver dose <13 GyE, and for liver metastasis treatment with 60 GyE in 3 fractions, liver constraints of V27 < 30%, V24 < 50%, and 700

ml receiving <15 GyE. Further evaluation is underway utilizing the equivalent uniform dose model to provide more accurate dose constraints.

Beam selection is critical in proton and heavy ion therapy as one must consider the stability of the WPL the particle will pass through to reach the target and distal edge placement. First, when considering the stability of the WPL, factors such as the edge of the immobilization device, abdominal motion, lung excursion, and bowel gas must be considered. Choosing beams that enter either entirely through the immobilization device or enter entirely avoiding the device are preferable. Beams that traverse the edge of the immobilization device can incur further range uncertainty due to daily shifts of the immobilization device relative to the target, placing more or less of the immobilization device in the beam path. Anterior beams are also avoided where possible, as abdominal motion creates an unstable external contour, and anterior beams tend to pass through abdominal gas creating WPL instability. At the JMSPTRC treatment plans are generated using two to three beams oriented through approximately a 90° arc between the right lateral and posterior positions that when combined with our immobilization techniques (i.e., POD) minimize variations in WPL, which minimize these variables (see Fig. 10.2).

Dome lesions also present a challenge in that respiratory motion can create large differences in WPL due to varying amount of lung in the field, however, reports show that this can be addressed through active breathing management or smearing techniques [22]. Smearing is a technique used to account for uncertainty in WPL due to target motion relative to other anatomy by smoothing out the proton distal edge profile. This is achieved by applying a smear radius to each point on the distal edge surface, with the larger the radius giving a greater level of smoothing. This method impacts the design of the compensator (or beam spot pattern in IMPT) resulting in a broadening and smoothing of the proton distal edge reducing conformity in this region. The goal of this is to ensure that errors involving inadequate distal range caused by shifts in WPL are minimized and target coverage is maintained.

Additionally, when choosing beam angles one must consider the relative biological effectiveness (RBE) of the distal edge of the proton beam. Proton therapy centers employ an RBE correction factor approximated to be 1.1 to dose delivered to the patient, however, near the distal edge of the Bragg peak LET increases markedly which can lead to increased biological damage in this region and even shift in the distal edge of the dose delivery [23]. The extent of biological enhancement in this region is uncertain as it depends on a number of factors including incident energy, LET distribution, cell type, biological endpoint, etc. This uncertainty is managed clinically by using beams that are largely orthogonal to avoid overlap of the distal portion of the Bragg peak, or by avoiding beams that stop on or near critical structures (GI structures in the case of targets in the liver) as these are most at risk from biological enhancement.

10.5 Beam Delivery

Proton and carbon ion beam depth dose distributions are characterized by a low entrance dose, followed by a high-dose peak (Bragg peak) at a predetermined depth governed by their initial energy and a sharp distal falloff (see Fig. 10.1) after which no primary particle dose is deposited. The superposition on multiple Bragg peaks of varying energy allows for the creation of a uniform dose area known as the spread out Bragg peak (SOBP) whose width can be customized to the target. This unique depth dose profile allows for conformal and homogeneous dose delivery to the target with fewer treatment beams (typically 2–3) and a lower integral dose to surrounding normal tissues (Fig. 10.2). The delivery of protons or carbon ions to the target is achieved through two distinct methods, passive scattering and pencil beam scanning.

Passive scattering typically utilizes a two-stage scattering system to create a wide proton beam of a given diameter for treatment [24]. The first stage of the scattering system is constructed from lead whose thickness is specified by a set of lead wedges [25] and is

customizable for varying beam energies/ranges. After passing through this scatterer the proton beam is Gaussian in profile with a FWHM of a few centimeters. The second stage of the scattering system is a contoured Lexan and lead disk whose profile is designed to be energy/field size specific and generate a uniform proton beam of given diameter. The Lexan thickness of the second scattering foil is complimentary to that of the lead component to ensure the proton beam range uniformity is maintained across the entire beam area [26]. The SOBP is generated by a rotating Lexan wheel with varying thickness steps to superimpose multiple Bragg peaks of varying range. Using this method SOBPs can be created with 0.5–1.0 cm resolution. The radiation is conformed to the target volume laterally by an aperture, made from brass or Cerrobend, and in depth through the use of a beam-specific compensator or bolus that is typically made from a low Z material such as wax or Lexan.

In pencil beam scanning beam delivery applications [27], the pencil beam from the accelerator is used directly to deliver dose to the target with no scattering. Instead the pencil beam is magnetically scanned over the target volume [28, 29] similar to airbrushing. The unmodulated Bragg peak creates a high dose spot at a given position within the target. These high dose spots are then moved laterally using magnetic positioning to deliver dose to a layer of the target at a given depth. When the planned dose to that specific layer has been delivered, the energy of the beam is then changed at the accelerator and dose is delivered to the next layer. This method of dose delivery allows for dose to be delivered homogeneously or inhomogeneously to the target (often referred to as intensity modulated proton therapy or IMPT [30]) with it possible to shape the lateral, distal, and proximal boundaries of the dose delivery without the need for an aperture or compensator.

The two methods of proton delivery are complimentary in their clinical application. Passive scattering with an aperture allows for proton beam delivery with improved penumbra over pencil beam scanning delivery with no aperture. However, the downside can be creation of the aperture and the necessity for this in passive scattered proton delivery can impact deliverable field size. Pencil beam scanning can allow for the treatment of larger fields (the size is limited by the strength of the scanning magnets but is often 40×40 cm^2) and shaping of both the proximal and distal sides of the SOBP. The flexibility of pencil beam scanning to deliver inhomogeneous and complex dose distributions also has potential clinical benefit in some cases. However, it must be noted that care needs to be taken when treating moving targets with pencil beam scanning. As pencil beam scanning and IMPT relies on accurate placement of the high-dose beam spot in three-dimensional space, as governed by the treatment plan, it can be susceptible to dose delivery errors if motion is not minimized through the use of immobilization or beam delivery techniques such as gating. Movement of the target during beam delivery and incorrect placement of the beam spot can lead to hot/cold dose spots within the target and potential irradiation of nontarget tissue. Passive scattering is much less susceptible to such errors as the target is treated uniformly with time and the lateral, distal, and proximal dose margins are created during the treatment planning process to account for tumor motion that is evaluated using 4DCT and potentially minimized using immobilization.

10.6 Treatment Facilities

Proton and carbon ion therapy facilities are characterized by a large central accelerator that provides high-energy particles to multiple treatment rooms [25]. The central accelerator is typically either a synchrotron or cyclotron. Synchrotrons generate a pulsed beam of protons or heavier ions, the energy of which can be varied at the accelerator level to meet the needs of the treatment team. This method produces a very monoenergetic beam of ions with minimal energy spread, yet the rate of beam delivery is typically fixed. Cyclotrons on the other hand produce a continuous beam of single maximum ion energy. Lower energies that may be required for treatment are then generated by passing the

ion beam through a variable range shifter that is located in close proximity to the accelerator to minimize transportation of secondary radiations to the treatment room. Cyclotron produced ion beams are characterized by a beam with increased energy spread, yet the rate of beam delivery can be increased by varying the beam current in the accelerator. The treatment rooms can employ either an isocentric 360° gantry, limited arc, or gantry fixed beam delivery using either passive scattering or pencil beam delivery techniques. The patient is located and immobilized on a positioner with 3–6 degrees of freedom and is aligned for treatment using digital X-ray images compared to digitally reconstructed radiographs generated during the treatment planning process. Single-room proton therapy systems are also becoming available which utilize compact gantry mounted cyclotron accelerators. These systems typically use a reduced gantry arc of rotation and employ a robotic patient positioner to achieve a wide range of treatment angles.

10.7 Out-of-Field Dose

As a result of radiation interactions with the beam delivery system and the patient secondary radiations such as electrons, photons, and neutrons can be produced that go on to deposit unwanted out-of-field dose to the patient. Of these radiations, neutrons pose the greatest concern due to their increased relative biological effectiveness [31]. The amount of out-of-field dose delivered to the patient is dependent on many factors including beam delivery technique, incident proton energy, and incident beam area to collimated beam area ratio. The extent of out-of-field dose has been investigated by a number of groups at various institutions [32–39] and is typically of the order of mSv/Gy near the treatment field with an exponential fall off to μSv/Gy 5–10 cm from the field edge [32]. It is important to also note that the out-of-field dose delivered by proton beam delivery is comparable to or less than that delivered from head scatter, head leakage, and patient scatter during IMRT or arc-based photon treatments [40]. An additional factor that contributes to out-of-field dose in heavy ion therapy (i.e., carbon therapy) is fragmentation of the treatment particle producing radiations that may go on to deliver dose beyond the distal edge of the Bragg peak. This will be discussed further in the next section.

10.8 Carbon Therapy

The rationale behind using heavier ions (such as Carbon or Oxygen) in clinical treatment is motivated by multiple factors, many of which are similar to the ones discussed for protons including a narrower Bragg peak with improved peak-to-entrance dose ratio, sharper penumbra, and potentially lower integral dose. Heavier ions have the additional benefits of an increased linear energy transfer (LET) and subsequent increase in RBE, currently estimated at 3 [41] for carbon, over protons (1.1) and x-rays (1). The higher LET means that increasing amounts of the damage done by carbon beams is through direct damage rather than through a secondary free radical mechanism and thus carbon ions also have less dependence on oxygenation. The hope is that higher LET accelerated ions such as carbon will increase cell killing in those tumors with hypoxia and cells with high rates of sublethal repair and/or high radioresistance to low LET radiation.

There are, however, a number of factors that have hampered the clinical deployment of heavy ion therapy into regular clinical practice. The first and perhaps biggest hurdle is the facility cost and complexity. Accelerating and directing heavier ions require larger diameter accelerators and larger magnets, resulting in larger/heavier gantries. These considerations not only impact the footprint of the facility but also the engineering and design to achieve precision of alignment which in turn elevates cost. While heavy ions exhibit advantages in physical dose distribution due to their size, fragmentation of the primary ion to lighter fragments can lead to dose delivery beyond the distal edge of the Bragg peak. This can negatively impact the dose sparing of a

heavy ion beam especially beyond the distal edge. Finally, heavy ions can vary significantly in their biological effectiveness along the depth dose profile requiring biologically effective dose to be the parameter used in planning. The data used in computing biologically effective dose can either be experimental based [42] or model based such as by the local effect model (LEM) [43, 44]. While this enhanced biological effectiveness increases cell killing in those tumors with hypoxia and cells with high rates of sublethal repair and/or high radioresistance to low LET radiation, additional biological validation and clinical trials with varying fractionation will increase clinical confidence in the technique.

10.9 Future Directions

As particle therapy continues to evolve we are seeing key work being completed in technical development, phase III clinical trials, and increased patient access. Technical improvements are focused on widening the therapeutic window for large tumors and tumors in difficult locations, while further increasing the conformity of the dose delivery. Maturing clinical trials will begin to provide quantitative data on the benefits of particle therapy in relation to other treatment modalities. Finally, a wider availability of particle therapy, including smaller, self-contained, and less expensive proton centers will provide increasing patient access to the benefits afforded by proton and particle therapy.

The technical advances envisaged for particle therapy focus on expanding the range of tumors that can be treated. In part, this advancement is shared with photon therapy, in that reductions in the ITV and PTV allow for less normal tissue to be treated. Reductions in the ITV can occur through improvements to patient immobilization, gated beam delivery, and tumor tracking. The use of implanted fiducials aids tumor localization, however, requires an invasive procedure and dose perturbation by the implanted material. To address dose perturbation carbon-coated, stainless steel fiducials or water equivalent fiducials could be employed, however, the problem of an invasive procedure still exists in patients who oftentimes have coagulopathies. Advanced fiducial or surface imaging technology could be employed to track target motion and in conjunction with beam gating technology ensure that beam delivery only occurs when the target is properly located. Cone beam CT (CBCT) also provides a potential for volumetric analysis of target placement in the treatment room and can possibly be employed in adaptive therapy. In adaptive therapy applications the CBCT images could be used along with deformable image registration and pencil beam scanning beam delivery to replan treatments addressing concerns which arise with ascites and variation in water path length that can oftentimes render these patients unsuitable for proton and particle therapy.

The treatment of liver tumors with particle therapy, while growing, is only reaching its adolescence. Current reports in the literature encompass retrospective [10–12, 45–50] and phase II clinical trials [4–8] and the current time is exciting in that the first phase III data including protons is set to emerge through several studies. The first is a phase III trial from JMSPTRC showing favorable interim results of proton therapy versus transarterial chemoembolization [51]. The second, RTOG 1112, is actively encouraging treatment of patients in the SBRT and Sorafenib arm with proton therapy. Analysis from these trials will aid in quantifying the benefits of proton therapy in the treatment of liver tumors.

As the physical, biological, and clinical benefits are becoming defined, providing access to this technology will remain a key issue. Patients require multiple treatments given on a daily or frequent basis, necessitating proximity to a treatment center. Recently, we have seen a significant rise in the number of proton therapy centers worldwide as the benefits of this modality of treatment are realized and technology improves. The development of single room proton centers provides at least part of the answer in widening the availability of this technology to the patient population. As the number of proton centers continues to rise, patients are

experiencing increased access to this modality and the physical, biological, and clinical benefits this provides.

10.10 Conclusion

Particle therapy is an enticing choice in the treatment of liver tumors, due to its ability to spare what often is an already poorly functioning liver through the use of the Bragg peak. However, as detailed within this chapter, special consideration must be taken with patient selection, treatment planning, and delivery so the level of precision seen on treatment plans can be translated into a deliverable dose to the patient. As shown in the phase II trials these challenges are being successfully met and thus the role of particle therapy, and in particular proton therapy, for the treatment of liver tumors will expand. As more patients are treated, increasing data will become available from which informed decisions can be made on when to employ particle therapy in the treatment of liver tumors.

References

1. Wilson RR. Radiological use of fast protons. Radiology. 1946;47:487–91.
2. Suit HD. Protons to replace photons in external beam radiation therapy? Clin Oncol. 2003;15:S29–31.
3. Engelsman M, Schwarz M, Dong L. Physics controversies in proton therapy. Sem Radiat Oncol. 2013;23:88–96.
4. Bush DA, Kayali Z, Grove R, Slater JD. The safety and efficacy of high-dose proton beam radiotherapy for hepatocellular carcinoma: a phase 2 prospective trial. Cancer. 2011;117:3053–9.
5. Fukumitsu N, Sugahara S, Nakayama H, et al. A prospective study of hypofractionated proton beam therapy for patients with hepatocellular carcinoma. Int J Radiat Oncol Biol Phys. 2009;74:831–6.
6. Hong TS, Wo JY, Yeap BY, et al. Multi-institutional phase ii study of high-dose hypofractionated proton beam therapy in patients with localized, unresectable hepatocellular carcinoma and intrahepatic cholangiocarcinoma. J Clin Oncology: Official Journal of the American Society of Clinical Oncology. 2016;34:460–8.
7. Kawashima M, Furuse J, Nishio T, et al. Phase II study of radiotherapy employing proton beam for hepatocellular carcinoma. J Clin Oncol: Official Journal of the American Society of Clinical Oncology. 2005;23:1839–46.
8. Nakayama H, Sugahara S, Fukuda K, et al. Proton beam therapy for hepatocellular carcinoma located adjacent to the alimentary tract. Int J Radiat Oncol Biol Phys. 2011;80:992–5.
9. Gandhi SJ, Liang X, Ding X, et al. Clinical decision tool for optimal delivery of liver stereotactic body radiation therapy: photons versus protons. Pract Radiat Oncol. 2015;5:209–18.
10. Sugahara S, Oshiro Y, Nakayama H, et al. Proton beam therapy for large hepatocellular carcinoma. Int J Radiat Oncol Biol Phys. 2010;76:460–6.
11. Hata M, Tokuuye K, Sugahara S, et al. Proton beam therapy for hepatocellular carcinoma patients with severe cirrhosis. Strahlentherapie und Onkologie: Organ der Deutschen Rontgengesellschaft [et al]. 2006;182:713–20.
12. Hata M, Tokuuye K, Sugahara S, et al. Proton beam therapy for hepatocellular carcinoma with portal vein tumor thrombus. Cancer. 2005;104:794–801.
13. Berthelsen AK, Dobbs J, Kjellen E, et al. What's new in target volume definition for radiologists in ICRU Report 71? How can the ICRU volume definitions be integrated in clinical practice? Cancer Imaging: The Official Publication of the International Cancer Imaging Society. 2007;7:104–16.
14. Wroe AJ, Bush DA, Schulte RW, Slater JD. Clinical immobilization techniques for proton therapy. Technol Cancer Res Treat. 2015;14:71–9.
15. Wroe A, Bush D, Slater J. Immobilization considerations for proton radiation therapy. Technol Cancer Res Treat. 2013.
16. Keane FK, Hong TS. Charged particle therapy for hepatocellular carcinoma: a commentary on a recently published meta-analysis. Ann Transl Med. 2015;3:365.
17. Cheung J, Kudchadker RJ, Zhu XR, Lee AK, Newhauser WD. Dose perturbations and image artifacts caused by carbon-coated ceramic and stainless steel fiducials used in proton therapy for prostate cancer. Phys Med Biol. 2010;55:7135–47.
18. Rydhog JS, Mortensen SR, Larsen KR, et al. Liquid fiducial marker performance during radiotherapy of locally advanced non small cell lung cancer. Radiother Oncol: Journal of the European Society for Therapeutic Radiology and Oncology. 2016.
19. Yang M, Zhu XR, Park PC, et al. Comprehensive analysis of proton range uncertainties related to patient stopping-power-ratio estimation using the stoichiometric calibration. Phys Med Biol. 2012;57:4095–115.
20. Paganetti H. Range uncertainties in proton therapy and the role of Monte Carlo simulations. Phys Med Biol. 2012;57:R99–117.
21. Dawson LA, Normolle D, Balter JM, McGinn CJ, Lawrence TS, Ten Haken RK. Analysis of radiation-induced liver disease using the Lyman NTCP model. Int J Radiat Oncol Biol Phys. 2002;53:810–21.

22. Pan X, Zhang X, Li Y, Mohan R, Liao Z. Impact of using different four-dimensional computed tomography data sets to design proton treatment plans for distal esophageal cancer. Int J Radiat Oncol Biol Phys. 2009;73:601–9.
23. Paganetti H, Goitein M. Radiobiological significance of beamline dependent proton energy distributions in a spread-out Bragg peak. Med Phys. 2000;27:1119–26.
24. Koehler AM, Schneider RJ, Sisterson JM. Flattening of proton dose distributions for large-field radiotherapy. Med Phys. 1977;4:297–301.
25. Lesyna D. Facility overview for a proton beam treatment center. Technol Cancer Res Treat. 2007;6:41–8.
26. Wroe AJ, Schulte RW, Barnes S, McAuley G, Slater JD, Slater JM. Proton beam scattering system optimization for clinical and research applications. Med Phys. 2013;40.
27. Lomax AJ, Albertini F, Boehringer T, et al. Spot scanning proton therapy: treatment planning and treatment verification. Radiother Oncol. 2006;78:S21-S.
28. Pedroni E. The new proton scanning gantry of PSI: a system designed for IMPT delivery in the whole body including moving targets. Radiother Oncol. 2006;78:S71-S.
29. Pedroni E, Bohringer T, Coray A, et al. Initial experience of using an active beam delivery technique at PSI. Strahlenther Onkol. 1999;175:18–20.
30. Lomax A, Albertini F, Bolsi A, et al. Intensity modulated proton therapy at PSI: things we have learnt (and are still learning). Radiother Oncol. 2005;76:S54–5.
31. Hall EJ. Intensity-modulated radiation therapy, protons, and the risk of second cancers. Int J Radiat Oncol Biol Phys. 2006;65:1–7.
32. Wroe A, Clasie B, Kooy H, Flanz J, Schulte R, Rosenfeld A. Out-of-field dose equivalents delivered by passively scattered therapeutic proton beams for clinically relevant field configurations. Int J Radiat Oncol Biol Phys. 2009;73:306–13.
33. Wroe A, Rosenfeld A, Schulte R. Out-of-field dose equivalents delivered by proton therapy of prostate cancer. Med Phys. 2007;34:3449–56.
34. Jarlskog CZ, Lee C, Bolch WE, Xu XG, Paganetti H. Assessment of organ-specific neutron equivalent doses in proton therapy using computational whole-body age-dependent voxel phantoms. Phys Med Biol. 2008;53:693–717.
35. Zheng Y, Newhauser W, Fontenot J, Taddei P, Mohan R. Monte Carlo study of neutron dose equivalent during passive scattering proton therapy. Phys Med Biol. 2007;52:4481–96.
36. Fontenot JD, Zheng Y, Taddei P, Newhauser W. Stray radiation exposure during proton radiotherapy of the prostate: the influence of the patient on scatter and production. Med Phys. 2007;34:2507.
37. Zheng Y, Newhauser W, Fontenot J, Taddei P, Mohan R. Study of neutron exposure during passively scattered proton therapy. Med Phys. 2007;34:2549–50.
38. Moyers MF, Benton ER, Ghebremedhin A, Coutrakon G. Leakage and scatter radiation from a double scattering based proton beamline. Med Phys. 2008;35:128–44.
39. Schneider U, Agosteo S, Pedroni E, Besserer J. Secondary neutron dose during proton therapy using spot scanning. Int J Radiat Oncol Biol Phys. 2002;53:244–51.
40. Hauri P, Halg R, Besserer J, Schneider U. General dose model for stray dose calculation of static and intensity-modulated photon radiation. Med Phys. 2016;43:1955–67.
41. Kato H, Tsujii H, Miyamoto T, et al. Results of the first prospective study of carbon ion radiotherapy for hepatocellular carcinoma with liver cirrhosis. Int J Radiat Oncol Biol Phys. 2004;59:1468–76.
42. Kanai T, Endo M, Minohara S, et al. Biophysical characteristics of HIMAC clinical irradiation system for heavy-ion radiation therapy. Int J Radiat Oncol Biol Phys. 1999;44:201–10.
43. Scholz M, Kellerer AM, Kraft-Weyrather W, Kraft G. Computation of cell survival in heavy ion beams for therapy. The model and its approximation. Radiat Environ Biophys. 1997;36:59–66.
44. Elsasser T, Kramer M, Scholz M. Accuracy of the local effect model for the prediction of biologic effects of carbon ion beams in vitro and in vivo. Int J Radiat Oncol Biol Phys. 2008;71:866–72.
45. Chiba T, Tokuuye K, Matsuzaki Y, et al. Proton beam therapy for hepatocellular carcinoma: a retrospective review of 162 patients. Clin Cancer Res: An Official Journal of the American Association for Cancer Research. 2005;11:3799–805.
46. Hashimoto T, Tokuuye K, Fukumitsu N, et al. Repeated proton beam therapy for hepatocellular carcinoma. Int J Radiat Oncol Biol Phys. 2006;65:196–202.
47. Hata M, Tokuuye K, Sugahara S, et al. Proton beam therapy for hepatocellular carcinoma with limited treatment options. Cancer. 2006;107:591–8.
48. Lee SU, Park JW, Kim TH, et al. Effectiveness and safety of proton beam therapy for advanced hepatocellular carcinoma with portal vein tumor thrombosis. Strahlentherapie und Onkologie: Organ der Deutschen Rontgengesellschaft [et al]. 2014;190:806–14.
49. Nakayama H, Sugahara S, Tokita M, et al. Proton beam therapy for hepatocellular carcinoma: The University of Tsukuba experience. Cancer. 2009;115:5499–506.

50. Sugahara S, Nakayama H, Fukuda K, et al. Proton-beam therapy for hepatocellular carcinoma associated with portal vein tumor thrombosis. Strahlentherapie und Onkologie: Organ der Deutschen Rontgengesellschaft [et al]. 2009;185:782–8.

51. Bush DA, Smith JC, Slater JD, et al. Randomized clinical trial comparing proton beam radiation therapy with transarterial chemoembolization for hepatocellular carcinoma: results of an interim analysis. Int J Radiat Oncol*Biol*Phys. 2016;95:477–82.